Magazine of Concrete Research
Volume 66 Issue 13

Crack propagation in concrete at very early ages
Dao, Morris and Dux

Magazine of Concrete Research, 2014, 66(13), 643–651
http://dx.doi.org/10.1680/macr.13.00205
Paper 1300205
Received 17/07/2013; revised 27/01/2014; accepted 03/02/2014
Published online ahead of print 24/04/2014

ice Institution of Civil Engineers publishing

Crack propagation in concrete at very early ages

Vinh T. N. Dao
Lecturer, School of Civil Engineering, University of Queensland, Brisbane, Queensland, Australia

Peter H. Morris
Adjunct Senior Fellow, School of Civil Engineering, University of Queensland, Brisbane, Queensland, Australia

Peter F. Dux
Emeritus Professor, School of Civil Engineering, University of Queensland, Brisbane, Queensland, Australia

Surface defects and cracks in early-age concrete slabs have been observed to propagate under adverse conditions, impairing the performance and service life of these structures. However, the underlying mechanism of this form of crack propagation has remained largely unexplained, with very limited literature available. In this paper, simple yet sufficiently rigorous theoretical analyses of crack propagation in early-age concrete slabs, based on combined geotechnical engineering and fracture mechanics models, are presented. The results obtained clearly show how surface cracks can become unstable and propagate further, and either become stable again or develop through the full depth of the slab. They also convincingly demonstrate the roles of surface cracks and defects, pore moisture suctions and exposure conditions in this process. Importantly, the critical role of good construction practices in minimising this form of cracking is highlighted. These include proper compaction and effective curing as well as timely and adequate saw-cutting.

Notation

D	depth of desiccation (m)
E	Young's modulus of concrete for normal stress (Pa)
G_F	fracture energy (J/m^2)
g	exponent of suction profile
H	Young's modulus of concrete for pore moisture pressure and suction (Pa)
K	stress intensity factor (N/m$^{3/2}$)
K_{cr}	fracture toughness for mode I cracking (N/m$^{3/2}$)
u_w	pore moisture pressure (Pa)
Z	depth below surface of slab (m)
γ_d	unit weight of desiccated concrete (N/m^3)
γ_s	unit weight of saturated concrete (N/m^3)
γ_w	unit weight of pore moisture (N/m^3)
ε_X	horizontal strain perpendicular to crack
ν	Poisson's ratio of concrete
σ_X	horizontal normal stress perpendicular to crack (Pa)
σ_Y	horizontal normal stress parallel to crack (Pa)
σ_Z	vertical normal stress (Pa)
Ψ_0	suction at surface of slab (Pa)
Ψ_Z	suction at depth Z below surface of slab (Pa)

Introduction

Surface defects and cracks may already exist or may develop in concrete slabs at ages from several hours after casting, especially when best construction practices for compaction and curing are not followed. These cracks may subsequently propagate to greater depths and, in extreme cases, extend completely through the thickness of the slab. This may seriously compromise the performance and service life of affected structures, resulting in possible severe economic consequences. It is therefore important that the underlying mechanisms of crack formation and propagation in early-age concrete, together with the critical factors influencing them, be well understood.

Unfortunately, in contrast to the relatively extensive publications on the crack formation mechanism (Cohen *et al.*, 1990; Dao, 2007; Morris and Dux, 2005a), the literature on crack propagation in early-age concrete and the factors influencing it is very limited. Morris and Dux (2003) appear to have first considered this for the case of linear suction profiles in semi-infinite slabs.

While it can be argued that the mechanism for crack propagation in mature concrete (Hillerborg *et al.*, 1976; Bazant, 2002) might be applicable for concrete at very early ages, this approach does not readily highlight the factors affecting the propagation process. An alternative approach that clearly demonstrates these influencing factors would help ensure their proactive and effective control, and thus minimise the likelihood of undesirable crack propagation.

This paper presents simple yet sufficiently rigorous theoretical analyses of crack propagation in concrete slabs at very early ages, based on combined geotechnical engineering and fracture mechanics models. The results obtained are used to show how initially shallow surface cracks can become unstable and propagate further, and either become stable again or develop through the full depth of the slab. The roles of surface cracks and defects,

pore moisture suctions and exposure conditions in crack propagation are also demonstrated. The critical role of good construction practices for compaction and curing in minimising this form of cracking is emphatically highlighted.

Solutions for crack depth

Application of linear elastic fracture mechanics

Cracks in early-age concrete tend to propagate by opening along their own axes and are often essentially planar over significant distances relative to the depth of the crack. In terms of the three fundamental modes of fracture mechanics (Figure 1), they are thus mode I cracks. In contrast, modes II and III respectively involve in-plane shearing and transverse tearing of the crack surfaces. The following analyses consider only a single mode I vertical crack in plane strain (Figure 2). The crack is assumed to propagate downwards from the surface of the concrete without interacting with other, similar cracks. In addition, the possible dynamic nature of crack propagation is not considered.

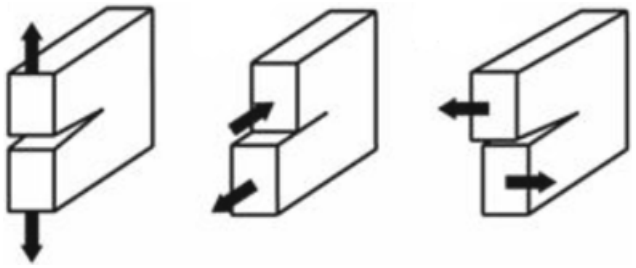

Figure 1. Basic modes of cracking

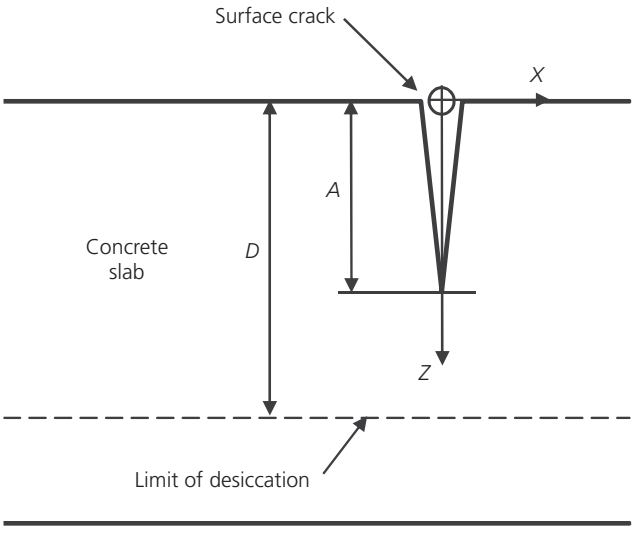

Figure 2. Definition sketch of concrete slab

Within the limitations of linear elastic fracture mechanics (LEFM), the crack depth for a given loading and geometry can be determined by simply equating the calculated stress intensity factor K (which is a function of the crack geometry and the stress distribution within the concrete) to a critical value K_{cr}, the fracture toughness (which is a function of several material parameters). Numerous solutions are available for simple stress distributions and crack geometries, and the rules for combining them are well known (Meguid, 1989; Wu and Carlsson, 1991). Here, stress intensity factors are calculated using the very versatile weight function method (Bueckner, 1970; Rice, 1972; Wu and Carlsson, 1991).

Strictly speaking, LEFM is applicable only to relatively large concrete structures in which the effect of the non-linear fracture process zone in front of the crack tip can be neglected (Bazant, 2002; Dao, 2007). However, any deviation of LEFM-based solutions from their true values can be accounted for by adjusting the corresponding values of K_{cr} (Morris *et al.*, 1994; Petersson, 1980). This approach has been used successfully for materials as ductile as mild steel (Orowan, 1955). The solutions presented here are thus at least semi-qualitatively valid.

Stresses in cracked plastic concrete

To determine crack depths using the weight function method, it is first necessary to calculate the stresses in the early-age concrete adjacent to the crack. The approach adopted here was to invoke Bueckner's principle (Bueckner, 1958), which states that the stress intensity factor for a stress-free crack (i.e. one with no loads on the crack faces) in a loaded body is identical to that for the same crack loaded internally with the stresses required to produce zero relative strain at the crack faces under the original loading. Since, in the simplified fracture mechanics model adopted, cracks are assumed to be stress-free, the problem of calculating the stresses adjacent to the crack is thus reduced to calculating the stresses at the crack location in an equivalent uncracked body.

Bueckner's principle, however, is inapplicable to problems in which the crack affects potential distributions, for example, a crack that is parallel to the initial direction of pore moisture flow (Morris *et al.*, 1994). Consequently, it is applicable to cracks in early-age concrete only if the cracks do not significantly affect the distribution of suctions (or pore moisture pressures) therein. The following analyses consider concrete slabs in which suctions are functions only of the depth below the slab surface. In real slabs, evaporation and flow of pore moisture from the crack faces as well as normal variability may cause the suctions to vary in plan as well as with depth.

Total stresses are considered and all stresses and pressures – including suctions – are based on the atmospheric datum (i.e.

atmospheric pressure is taken as zero) (Morris and Dux, 2005b). The usual convention of geotechnical engineering is followed; that is, compressive interparticle stresses and pore pressures are taken as positive. However, although suctions are negative pore pressures, for convenience they too are taken as numerically positive. No distinction is drawn between the effects of matric and osmotic suctions, although the effects of the latter in early-age concrete appear negligible (Dao *et al.*, 2011).

The following also apply.

- Desiccation due to hydration and the associated matric suction are, unless noted otherwise, assumed negligible.
- The stress due to pore moisture suction is equal to the suction. This assumption is correct only if the concrete is saturated or almost saturated (Morris and Dux, 2006). It is not, however, critical to the outcome of the analyses.
- The concrete is isotropic and elastic and remains so even if the strains are forced to be one-dimensional.

The horizontal strain perpendicular to the crack (Figure 2) is then given by (Morris *et al.*, 1992)

$$\varepsilon_X = \frac{\sigma_X}{E} - \frac{\nu}{E}(\sigma_Y + \sigma_Z) - \frac{u_w}{H} \quad (1)$$

Separate Young's moduli are defined in Equation 1 for the responses of the early-age concrete to normal stresses and to pore moisture pressures and suctions because it has not yet been established that a single modulus is sufficient (Morris *et al.*, 1992). If the concrete reacts in the same way to normal stresses and the essentially isotropic pore moisture pressures and suctions (Morris *et al.*, 1992) then

$$\frac{E}{H} = 1 - 2\nu \quad (2)$$

Prior to cracking, the stresses and strains in the concrete are essentially one-dimensional. That is, the normal stresses perpendicular and parallel to the crack are equal and the corresponding strains are both zero. Combining Equations 1 and 2 then gives

$$\sigma_X = \left(\frac{\nu}{1-\nu}\right)\sigma_Z + \left(\frac{1-2\nu}{1-\nu}\right)u_w \quad (3)$$

For depths less than the depth of desiccation (at which, by definition, the suction is zero), Equation 3 becomes

$$\sigma_X = \left(\frac{\nu}{1-\nu}\right)\gamma_d Z - \left(\frac{1-2\nu}{1-\nu}\right)\Psi_Z \quad (4)$$

For depths greater than the depth of desiccation, Equation 3 becomes

$$\sigma_X = \left(\frac{\nu}{1-\nu}\right)[\gamma_d D + \gamma_s(Z-D)] - \left(\frac{1-2\nu}{1-\nu}\right)\gamma_w(Z-D) \quad (5)$$

Suction profiles

The suction profiles that develop in initially saturated concrete desiccating monotonically from an exposed surface can be represented by Equation 6 for depths less than the depth of desiccation and Equation 7 below the depth of desiccation (Morris and Dux, 2005b)

$$\Psi_Z = \Psi_0\left(1 - \frac{Z}{D}\right)^g \quad (6)$$

$$\Psi_Z = -\gamma_w(Z-D) \quad (7)$$

The exponent g in Equation 6 may range from zero to infinity (Figure 3). Values of g of 0, 1, 2, 3 and 4 correspond to a uniform, linear, quadratic, cubic and quartic suction profile respectively. A g value of infinity corresponds to the limiting profile with a finite suction value at the exposed surface of the concrete and zero suction over the remainder of the profile. The lower the exponent g, the more severe the exposure condition.

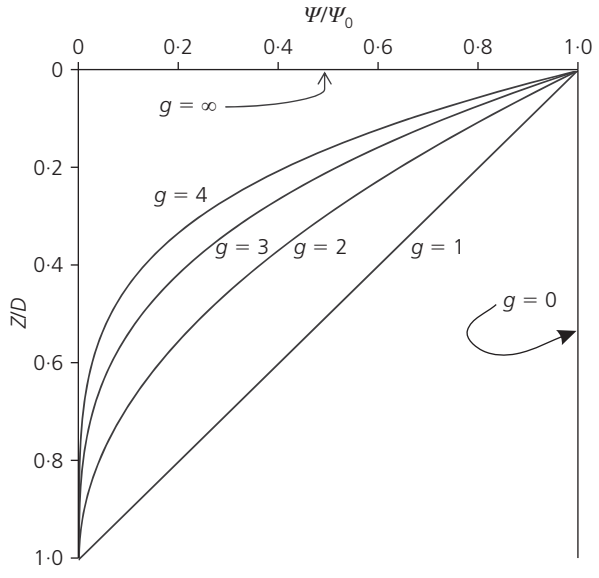

Figure 3. Suction profiles above depth of desiccation

The uniform profile ($g = 0$) represents low-slump (45 ± 10 mm) concrete that is desiccated both prior to and immediately following placement, before evaporation from the exposed upper surface becomes significant. Such concretes are often used in highway slabs to minimise the requirement for formwork (Kim *et al.*, 2014).

The concave quartic suction profile ($g = 4$) is considered to best represent concrete with a normal slump that was initially effectively fully saturated and is desiccating from its upper surface (Benson and Sill, 1991; Wong, 2007).

If the surface of the slab is fully desiccated, the suction at the surface equals atmospheric suction, while the matric suction at the depth of desiccation equals zero, corresponding to 100% saturation. Below the depth of desiccation, the pore pressure (a negative suction) is hydrostatic.

Variation of stress intensity factor with depth

Analytical expressions for the stress intensity factor K as a function of crack depth have been obtained for finite and semi-infinite slabs for crack depths both less than and greater than the depth of desiccation. The expressions for semi-infinite slabs for crack depths greater than the depth of desiccation and for all finite slabs are much too lengthy to present here. However, it will be shown later in the paper that the corresponding graphical solutions to special cases presented in Figures 4 to 10 can be used to obtain solutions for a wide range of input values.

The expressions for semi-infinite slabs for crack depths less than the depth of desiccation (Figure 2) are, however, relatively simple. Those for uniform, linear and concave quartic suction profiles (Figure 3) are given by Equations 8, 9 and 10 respectively

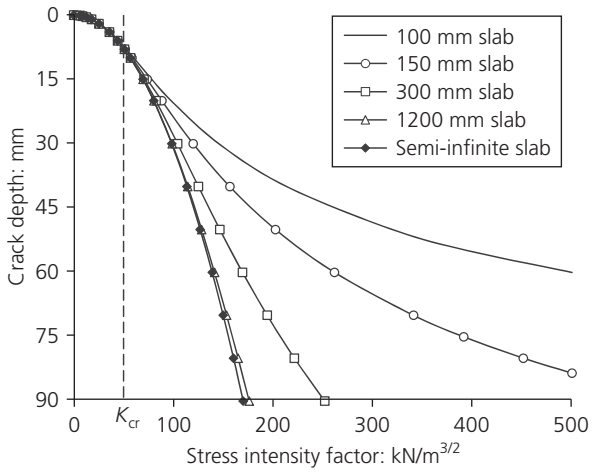

Figure 4. Variation of K with crack depth for uniform suction of 0·5 MPa over full depth of slab

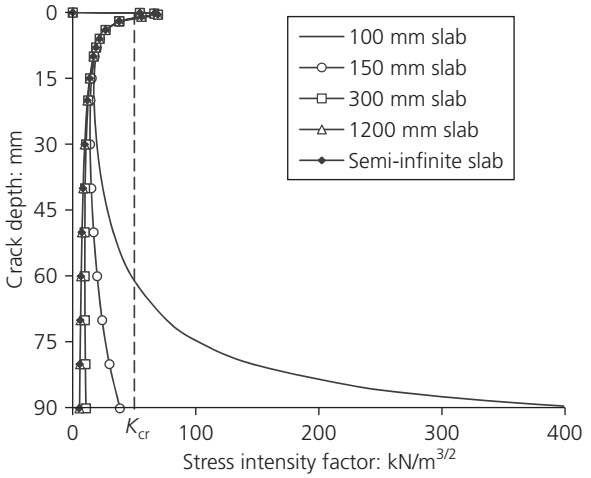

Figure 5. Variation of K with crack depth for concave quartic suction profile over uppermost 2 mm depth of slab and 5 MPa suction at surface

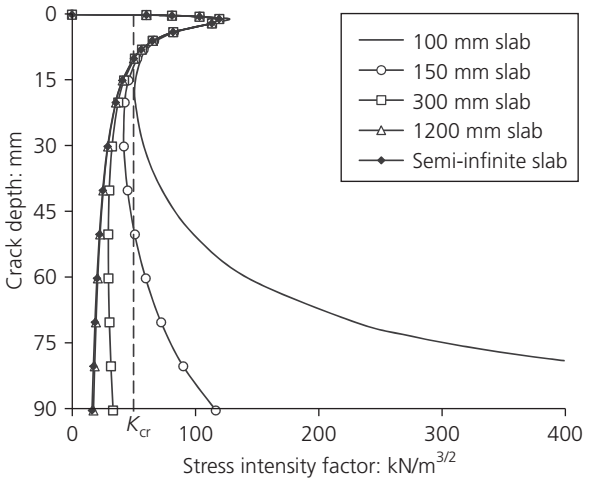

Figure 6. Variation of K with crack depth for concave quartic suction profile over uppermost 6 mm depth of slab and 5 MPa suction at surface

$$K = 1{\cdot}9878\left(\frac{1-2\nu}{1-\nu}\right)\Psi_0 A^{0{\cdot}5} - 1{\cdot}2088\left(\frac{\nu}{1-\nu}\right)\gamma_d A^{1{\cdot}5} \quad (8)$$

$$K = 1{\cdot}9878\left(\frac{1-2\nu}{1-\nu}\right)\Psi_0 A^{0{\cdot}5} - 1{\cdot}2088\left[\left(\frac{1-2\nu}{1-\nu}\right)\frac{4\Psi_0}{D} + \left(\frac{\nu}{1-\nu}\right)\gamma_d\right]A^{1{\cdot}5} \quad (9)$$

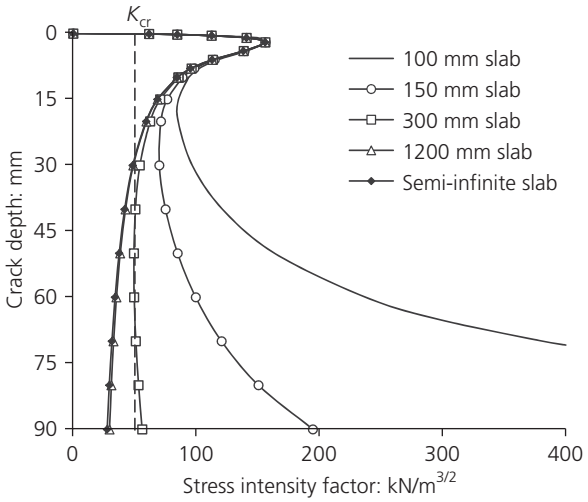

Figure 7. Variation of K with crack depth for concave quartic suction profile over uppermost 10 mm depth of slab and 5 MPa suction at surface

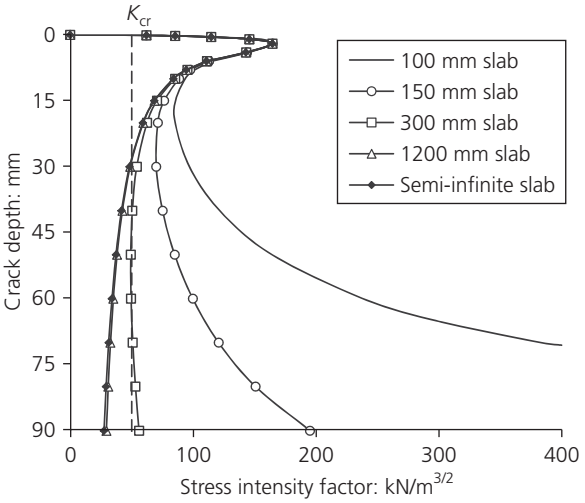

Figure 9. Variation of K with crack depth for concave quadratic suction profile over uppermost 6 mm depth of slab and 5 MPa suction at surface

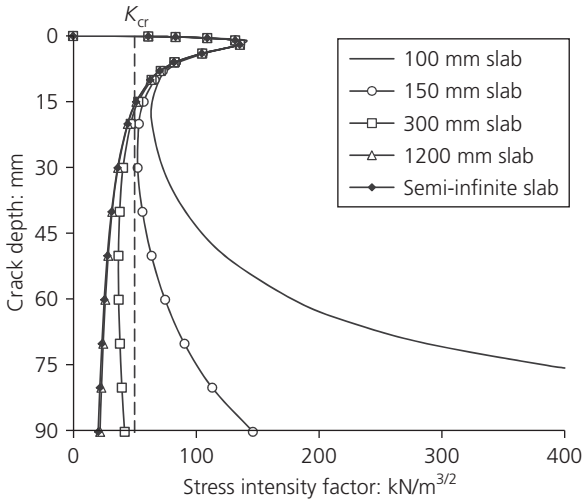

Figure 8. Variation of K with crack depth for concave cubic suction profile over uppermost 6 mm depth of slab and 5 MPa suction at surface

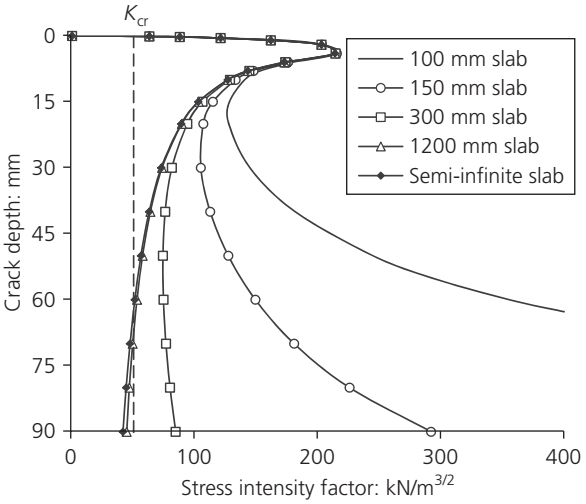

Figure 10. Variation of K with crack depth for linear suction profile over uppermost 6 mm depth of slab and 5 MPa suction at surface

$$K = 1{\cdot}9878\left(\frac{1-2\nu}{1-\nu}\right)\Psi_0 A^{0{\cdot}5} - 1{\cdot}2088\left[\left(\frac{1-2\nu}{1-\nu}\right)\frac{4\Psi_0}{D} + \left(\frac{\nu}{1-\nu}\right)\gamma_d\right]A^{1{\cdot}5} + 5{\cdot}5778\left(\frac{1-2\nu}{1-\nu}\right)\frac{\Psi_0}{D^2}A^{2{\cdot}5} - 3{\cdot}1195\left(\frac{1-2\nu}{1-\nu}\right)\frac{\Psi_0}{D^3}A^{3{\cdot}5} + 0{\cdot}6840\left(\frac{1-2\nu}{1-\nu}\right)\frac{\Psi_0}{D^4}A^{4{\cdot}5} \quad (10)$$

Fracture toughness

The critical stress intensity factor K_{cr} is termed the fracture toughness. For cracking in plane strain it is given by (Meguid, 1989; Irwin, 1957)

$$K_{cr} = \left(\frac{2G_F E}{1-\nu^2}\right)^{0{\cdot}5} \quad (11)$$

Input parameter values

The primary input parameters required to determine crack depths using the equations presented above are the fracture toughness

and Poisson's ratio of early-age concrete, the bulk densities of saturated and desiccated concrete and of the pore moisture, the suction at the surface of the concrete and the depth of desiccation.

- The fracture toughness can be estimated using Equation 11 and existing data for Young's modulus, Poisson's ratio and the fracture energy of early-age concrete (Dao, 2007). It has been shown in tensile strength tests that the Young's modulus of concrete increases from zero at the start of mixing to about 600 MPa after 6·5 h (Dao *et al.*, 2009). Values up 28 000 MPa (Kovler, 1994; Oluokun *et al.*, 1991) have been recorded at 12 h. The Young's modulus of cement paste varies from zero to 10 MPa at 8 h (Boumiz *et al.*, 1996).
- Poisson's ratio of concrete decreases from 0·5 immediately after mixing to about 0·2 when the degree of hydration reaches 10% (De Schutter and Taerwe, 1996; Oluokun *et al.*, 1991; Ouldhammou *et al.*, 1990). Poisson's ratio of early-age cement pastes similarly varies from 0·49 to 0·28 (Boumiz *et al.*, 1996).
- The fracture energy of early-age concrete increases over time from zero initially to about 80 J/m^2 at 6·5 h after mixing (Dao *et al.*, 2009). The fracture energy of cement mortars at ages 2·2–6·4 h assumes a similar range of values (Morris and Dux, 2005b).

On the basis of the foregoing, representative values of 70 MPa, 0·30 and 16 J/m^2 were adopted for Young's modulus, Poisson's ratio and the fracture energy of early-age concrete respectively. These three values together correspond to a fracture toughness of approximately 50 kN/m$^{3/2}$ (Equation 11). This is comparable to the fracture toughness of mature concrete, which is typically in the range 50–100 kN/m$^{3/2}$ (Bosco *et al.*, 1990; Carpinteri, 1981; Crisfield, 1986).

In the absence of experimental data on the effects of desiccation on the density of early-age concrete, a value of 23 kN/m^3 was used for both saturated and unsaturated concrete. The density of the pore moisture was taken to be 10 kN/m^3.

The solutions for crack depth were based on values for the suction at the surface of the concrete of 0·5 MPa and 5 MPa for low-slump and normal-slump concrete respectively. These suction values are based on limited but reasonably representative laboratory data obtained using a pychrometer and a leaf hygrometer. At 20°C, they correspond to relative humidities in the pores in the concrete of 99·6% and 96·4% respectively (Morris and Dux, 2005b; Philip, 1957). They are significantly lower than typical atmospheric suctions, which can readily reach values approaching 100 MPa or even higher (Morris and Dux, 2005b, 2006).

Depths of desiccation of 2, 6 and 10 mm were considered. For initially saturated concrete with a representative void ratio (volume of voids divided by volume of solids) of 0·2 and an evaporation rate of 1 (kg/m^2)/h (ACI, 2001), these values correspond to delays of 20, 60 and 100 min following the evaporation of the last of the bleed water, if any, to empty the voids completely. The time taken for the surface concrete to become only partially saturated would be significantly less.

Solutions for crack propagation in early-age concrete

The solutions for crack depth based on the foregoing analyses are presented in Figures 4 to 10 for slabs ranging in thickness from 100 mm to 1200 mm. The solutions are presented and discussed in terms of the representative values of fracture toughness (50 kN/m$^{3/2}$) and surface suctions (0·5 MPa and 5 MPa) nominated above.

In Figures 4 to 10, the critical condition required for cracking is represented by the vertical dotted line of fracture toughness K_{cr}

- cracks with depths that have a corresponding stress intensity factor K less than K_{cr} of 50 kN/m$^{3/2}$ will remain stable
- cracks with depths having corresponding K greater than K_{cr} will be unstable and will propagate.

Solutions for uniform suction profile

Figure 4 shows the solutions for a stress intensity factor corresponding to a uniform suction of 0·5 MPa over the full depth of the slab, which, as noted earlier, represents a low-slump concrete for highway slabs immediately after placing. For all slabs, the stress intensity factor increases monotonically with increasing crack depth.

It can be readily observed that cracks and pre-existing defects with depths of less than about 8 mm have corresponding K values less than K_{cr} and will thus remain stable. Deeper cracks will propagate through the full thickness of the slab.

Solutions for concave quartic suction profiles

Figures 5–7 show the solutions for crack depth corresponding to concave quartic suction profiles ($g = 4$ in Figure 3) with 5 MPa surface suction and depths of desiccation of 2, 6 and 10 mm respectively. As noted earlier, these profiles represent normal-slump concrete that is allowed to desiccate from the exposed surface after placing. Unlike the stress intensity factors in the case of a uniform suction profile (Figure 4), those in Figures 5–7 do not increase monotonically with crack depth. Comparison of the three figures shows that, although the overall form of the solutions does not change, the crack depths increase with increasing depth of desiccation.

Figure 5 indicates that for a depth of desiccation of 2 mm and the other input values considered, the stress intensity factor of surface defects approximately 0·1 mm in depth exceeds the fracture toughness. Consequently, surface defects of that size or slightly larger will propagate. For all slabs, however, the stress intensity factor falls below the critical value K_{cr} of 50 kN/m$^{3/2}$ for cracks deeper than approximately 1·5 mm. Crack propagation consequently stops

at this depth and will not resume unless either the surface suction or the depth of desiccation increases. However, the stress intensity factor for the 100 mm slab again exceeds the fracture toughness for surface defects that are 61 mm or deeper. Any of the latter will thus propagate through the full depth of the slab. Deeper cracks or defects are necessary to produce the same result in thicker slabs.

The solutions for depths of desiccation of 6 mm and 10 mm (Figures 6 and 7) are similar to those for the 2 mm depth (Figure 5). Very small surface defects can, however, propagate through the full thickness of the 100 mm slab for a desiccation depth of 6 mm (Figure 6) and through both the 100 mm and 150 mm slabs for a depth of desiccation of 10 mm (Figure 7).

Solutions for other suction profiles

Figures 8–10 show the solutions for crack depth for concave cubic, concave quadratic and linear suction profiles (which correspond to g values of 3, 2 and 1 respectively (Figure 3)) with 5 MPa suction at the surface and a depth of desiccation of 6 mm in all cases. As noted earlier, a lower value of g corresponds to a more severe exposure condition. It can be seen that, as the profile changes from concave quartic (Figure 6) to concave cubic, quadratic and linear (Figures 8–10), the overall form of the solutions is unchanged, but the crack depths corresponding to a given stress intensity factor increase progressively.

Accounting for variations in input parameters

The effect on the solutions of surface suction values other than the 0·5 MPa and 5 MPa used to plot Figures 4–10 can be accounted for as follows. In the figures, the solutions for semi-infinite slabs do not differ significantly from the corresponding solutions for the 1200 mm slabs, which, for the input variables considered can thus be considered effectively semi-infinite. For the 1200 mm slabs, the maximum vertical stress due to the self-weight of the concrete is approximately 28 kPa, which corresponds to only 5·5% and 0·6% respectively of the 0·5 MPa and 5 MPa surface suctions considered. That is, for any realistic depth of desiccation, the solutions for crack depth are dominated by the surface suction values. The fracture toughness is thus, to a good approximation, directly proportional to the surface suction (Equations 8–10) and the effect of varying the latter can thus be determined simply by varying the fracture toughness scales in Figures 4–10 in linear proportion. The effect on the solutions shown in Figures 4–10 of varying the fracture toughness can be determined simply by relocating the fracture toughness lines accordingly.

Variations of the depth of desiccation in the solutions plotted in Figures 5–10 cannot be accounted for by simple graphical methods; it is necessary to produce a new plot in each case. (The depth of desiccation is not a variable in the solutions shown in Figure 4.) However, Figures 5–7, which show the solutions for the concave quartic suction profile (the most likely to be encountered in practice), cover the range of depth of desiccation (2–10 mm) likely to arise in practice. Figures 8–10, which are all plotted for a depth of desiccation of 6 mm only, correspond to less likely desiccation profiles.

Discussion

Close examination of the solutions presented in Figures 4–10 shows the following.

(*a*) The more adverse the exposure condition, the more severe the consequences.
  (*i*) For the 150 mm thick slabs in Figures 5–7, surface defects of 5 mm depth are stable for a depth of desiccation of 2 mm (Figure 5) but would propagate to a depth of about 10 mm for an increased depth of desiccation of 6 mm (Figure 6). When the depth of desiccation becomes 10 mm due to an even higher rate of surface evaporation of water under more severe exposure conditions (Figure 7), any small surface defects would trigger full-depth cracking, resulting in serious random cracking.
  (*ii*) Considering the 300 mm thick slabs in Figures 6 and 10: for the case of a concave quartic suction profile ($g = 4$) (Figure 6), surface defects deeper than 10 mm are associated with $K < K_{cr}$ and are thus stable. Any shallower surface defect would propagate but be arrested at this stable depth of 10 mm. However, under the more adverse condition of a linear suction profile ($g = 1$) (Figure 10), any surface defect is unstable and would propagate to full depth.

(*b*) The deeper the surface cracks/defects, the more severe the consequences.
  (*i*) Taking the 150 mm thick slab in Figure 6 as an illustration, shallow surface defects would propagate to a depth of about 10 mm and then stabilise. They may also extend along the surface but would not grow deeper. Defects of between 10 mm and 50 mm depth would also be stable for this slab under the given conditions. However, defects deeper than about 50 mm would develop into full-depth cracks.
  (*ii*) This has important implications for sawn joints, which are essentially purposely introduced surface cracks at pre-determined locations to minimise undesirable random cracking: the sawn joints have to be deeper than other existing surface defects to ensure crack propagation would occur at these joints but not elsewhere.

The above discussion clearly highlights the critical role of good construction practices, including

- proper compaction to minimise the size and amount of surface defects
- effective curing to protect the concrete surface from adverse exposure conditions and to promote optimal hydration (and hence a desirable increased K_{cr})
- timely and sufficiently deep saw-cutting to create dominant

defects so that cracking with associated stress relief occurs as planned.

Summary and conclusions

Simple yet sufficiently rigorous analytical and graphical solutions for the depth of cracking in desiccating early-age concrete slabs have been presented. These solutions have then been applied to explain how surface cracks in early-age concrete can become unstable and propagate further, and either become stable again or develop through the full depth of the slab.

Simple methods have also been presented that enable the graphical solutions to be adapted to account for different values of surface suction and critical fracture toughness. No such adjustments can account for variations in the pore moisture suction profile or the depth of the desiccated layer at the exposed surface of the concrete, but the plots presented cover the whole range of these parameters likely to be encountered in practice.

This paper clarifies the effects of surface cracks/defects, pore moisture suctions and exposure conditions in this process. Importantly, the critical role of good construction practices is clearly highlighted, including proper compaction, effective curing, and timely and adequate saw-cutting.

REFERENCES

ACI (American Concrete Institute) (2001) ACI 308R-01: Guide to curing concrete. American Concrete Institute, Farmington Hills, MI, USA.

Bazant ZP (2002) Concrete fracture models: testing and practice. *Engineering Fracture Mechanics* **69(2)**: 165–205.

Benson RE and Sill BL (1991) Evaporative drying of dredged material. *ASCE Journal of Waterway, Port, Coastal and Ocean Engineering* **117(3)**: 216–235.

Bosco C, Carpinteri A and Debernardi PG (1990) Fracture of reinforced concrete: scale effects and snap-back instability. *Engineering Fracture Mechanics* **35(4–5)**: 665–677.

Boumiz A, Vernet C and Cohen Tenoudji F (1996) Mechanical properties of cement pastes and mortars at early ages. *Advanced Cement Based Materials* **3(3–4)**: 94–106.

Bueckner HF (1958) The propagation of cracks and the energy of elastic deformation. *Transactions of the American Society of Mechanical Engineers* **80(6)**: 1225–1230.

Bueckner HF (1970) A novel principle for the computation of stress intensity factors. *Zeitschrift fur Angewandte Mathematik und Mechanik* **50(9)**: 529–546.

Carpinteri A (1981) Static and energetic fracture parameters for rocks and concretes. *Materials and Structures* **14(81)**: 151–162.

Cohen MD, Olek J and Dolch WL (1990) Mechanism of plastic shrinkage cracking in Portland cement and Portland cement–silica fume paste and mortar. *Cement and Concrete Research* **20(1)**: 103–119.

Crisfield MA (1986) Snap-through and snap-back response in concrete structures and the dangers of under-integration. *International Journal for Numerical Methods in Engineering* **22(3)**: 751–767.

Dao VTN (2007) *Early-Age Cracking of Concrete*. PhD thesis, University of Queensland, Brisbane, Queensland, Australia.

Dao VTN, Dux PF and Morris PH (2009) Tensile properties of early-age concrete. *ACI Materials Journal* **106(6)**: 1–10.

Dao VTN, Morris PH and Dux PF (2011) Plastic shrinkage cracking of concrete – roles of osmotic suction. *Magazine of Concrete Research* **63(10)**: 743–750.

De Schutter G and Taerwe L (1996) Degree of hydration-based description of mechanical properties of early age concrete. *Materials and Structures* **29(190)**: 335–344.

Hillerborg A, Modeer M and Petersson PE (1976) Analysis of crack formation and crack growth in concrete by means of fracture mechanics and finite elements. *Cement and Concrete Research* **6(6)**: 773–781.

Irwin GR (1957) Analysis of stresses and strains near the end of a crack traversing a plate. *Journal of Applied Mechanics* **24**: 361–364.

Kim SH, Park JY and Jeong JH (2014) Effect of temperature-induced load on airport concrete pavement behavior. *KSCE Journal of Civil Engineering* **18(1)**: 182–187.

Kovler K (1994) Testing system for determining the mechanical behaviour of early age concrete under restrained and free uniaxial shrinkage. *Materials and Structures* **27(170)**: 324–330.

Meguid SA (1989) *Engineering Fracture Mechanics*. Elsevier, London, UK.

Morris PH and Dux PF (2003) Cracking of plastic concrete. *Australian Journal of Civil Engineering* **1(1)**: 17–21.

Morris PH and Dux PF (2005a) A review of ACI recommendations for prevention of plastic cracking. *ACI Materials Journal* **102(5)**: 307–314.

Morris PH and Dux PF (2005b) Suctions, fracture energy, and plastic cracking of cement mortar and concrete. *ACI Materials Journal* **102(6)**: 390–396.

Morris PH and Dux PF (2006) Crack depths in desiccating plastic concrete. *ACI Materials Journal* **103(2)**: 90–96.

Morris PH, Graham J and Williams DJ (1992) Cracking in drying soils. *Canadian Geotechnical Journal* **29(2)**: 263–277.

Morris PH, Graham J and Williams DJ (1994) Crack depths in drying clays using fracture mechanics. In *Fracture Mechanics Applied to Geotechnical Engineering*. ASCE Special Publication 43. ASCE, New York, USA, pp. 40–53.

Oluokun FA, Burdette EG and Deatherage JH (1991) Elastic modulus, Poisson's ratio, and compressive strength relationships at early ages. *ACI Materials Journal* **88(1)**: 3–10.

Orowan E (1955) Energy criteria of fracture. *Welding Journal* **34(3)**: 157–160.

Ouldhammou L, Okoh PN and Baudeau P (1990) Mechanical properties of fresh concrete before setting. In *Proceedings of International Conference on Rheology of Fresh Cement and Concrete* (Banfill PFG (ed.)). Spon, Liverpool, UK, pp. 249–258.

Petersson PE (1980) Fracture energy of concrete: method of determination. *Cement and Concrete Research* **10(1)**: 79–89.

Philip JR (1957) Evaporation, and moisture and heat fields in the soil. *Journal of Meteorology* **14(4)**: 354–366.

Rice JR (1972) Some remarks on elastic crack-tip stress fields. *International Journal of Solids and Structures* **8(6)**: 751–758.

Wong LT (2007) *Modification of Dredged Sediments to Produce Useful Products by Heating to High Temperatures*. PhD thesis, University of Queensland, Brisbane, Queensland, Australia.

Wu XR and Carlsson AJ (1991) *Weight Functions and Stress Intensity Factor Solutions*. Pergamon, Oxford, UK.